Original Investigation

Large-Scale Brain Network Coupling Predicts Acute Nicotine Abstinence Effects on Craving and Cognitive Function

Caryn Lerman, PhD; Hong Gu, PhD; James Loughead, PhD; Kosha Ruparel, MSE; Yihong Yang, PhD; Elliot A. Stein, PhD

Editorial page 491

IMPORTANCE Interactions of large-scale brain networks may underlie cognitive dysfunctions in psychiatric and addictive disorders.

OBJECTIVES To test the hypothesis that the strength of coupling among 3 large-scale brain networks—salience, executive control, and default mode—will reflect the state of nicotine withdrawal (vs smoking satiety) and will predict abstinence-induced craving and cognitive deficits and to develop a resource allocation index (RAI) that reflects the combined strength of interactions among the 3 large-scale networks.

DESIGN, SETTING, AND PARTICIPANTS A within-subject functional magnetic resonance imaging study in an academic medical center compared resting-state functional connectivity coherence strength after 24 hours of abstinence and after smoking satiety. We examined the relationship of abstinence-induced changes in the RAI with alterations in subjective, behavioral, and neural functions. We included 37 healthy smoking volunteers, aged 19 to 61 years, for analyses.

INTERVENTIONS Twenty-four hours of abstinence vs smoking satiety.

MAIN OUTCOMES AND MEASURES Inter-network connectivity strength (primary) and the relationship with subjective, behavioral, and neural measures of nicotine withdrawal during abstinence vs smoking satiety states (secondary).

RESULTS The RAI was significantly lower in the abstinent compared with the smoking satiety states (left RAI, $P = .002$; right RAI, $P = .04$), suggesting weaker inhibition between the default mode and salience networks. Weaker inter-network connectivity (reduced RAI) predicted abstinence-induced cravings to smoke ($r = -0.59$; $P = .007$) and less suppression of default mode activity during performance of a subsequent working memory task (ventromedial prefrontal cortex, $r = -0.66$, $P = .003$; posterior cingulate cortex, $r = -0.65$, $P = .001$).

CONCLUSIONS AND RELEVANCE Alterations in coupling of the salience and default mode networks and the inability to disengage from the default mode network may be critical in cognitive/affective alterations that underlie nicotine dependence.

Author Affiliations: Center for Interdisciplinary Research on Nicotine Addiction, Department of Psychiatry, University of Pennsylvania, Philadelphia (Lerman, Loughead); Intramural Research Program, National Institute on Drug Abuse, Baltimore, Maryland (Gu, Yang, Stein); Brain Behavior Laboratory, Department of Psychiatry, University of Pennsylvania, Philadelphia (Ruparel).

Corresponding Author: Caryn Lerman, PhD, Center for Interdisciplinary Research on Nicotine Addiction, Department of Psychiatry, University of Pennsylvania, 3535 Market St, Ste 4100, Philadelphia, PA 19104 (clerman@upenn.edu).

JAMA Psychiatry. 2014;71(5):523-530. doi:10.1001/jamapsychiatry.2013.4091
Published online March 12, 2014.

Cognitive dysfunction is a core component of neuropsychiatric and addictive disorders. With nicotine dependence, specific deficits in working memory (WM) emerge during nicotine withdrawal[1-3] and promote smoking relapse.[4,5] These deficits are accompanied by reduced activation in executive control regions (eg, the dorsolateral prefrontal cortex [DLPFC]) and less suppression of activation in task-independent regions (eg, the posterior cingulate cortex [PCC]).[6-9]

These patterns of regional activity are also reflected in fluctuations in large-scale brain networks at rest.[10-13] The following 3 networks have received the most attention: an executive control network (ECN) implicated in attention to and processing of exogenous stimuli; a default mode network (DMN) involved in stimulus-independent thought processes (eg, self-referential thinking); and a salience network (SN) facilitating orientation to external vs internal stimuli and allocating attention.[10,14-18] Evidence suggests a negative correlation between ECN and DMN activities[19,20] and a role for the SN in modulating relative activity in the ECN vs DMN.[18,21]

Sutherland and colleagues[22] recently proposed that, in the nicotine-deprived state, the SN allocates enhanced attentional resources toward internal symptoms of withdrawal, thereby biasing activity toward the DMN and away from the ECN. Given the hypothesized role of the SN in toggling resources between the ECN and DMN, a composite quantitative network association index integrating the SN-ECN (positive) correlation and the SN-DMN (negative) correlation, referred to as the *resource allocation index* (RAI), is proposed to assess nicotine withdrawal effects on this triple network interaction. We examined the RAI in smokers undergoing functional magnetic resonance imaging after 24 hours of abstinence and smoking satiety[6] and tested the hypotheses that the RAI would (1) be weaker in the abstinent compared with the smoking states, (2) predict abstinence-induced changes in craving, and (3) predict abstinence-induced impairments in cognitive performance and neuronal activation.

Methods

Participants

Fifty-four smokers (≥10 cigarettes per day for ≥6 months) gave written informed consent as approved by the University of Pennsylvania institutional review board. Subjects were required to be 18 to 65 years of age and right-handed, with no history of brain trauma or *DSM-IV* Axis I psychiatric disorders or substance (except nicotine) dependence.[23] Exclusion criteria consisted of use of other tobacco or cessation products, pregnancy, and IQ scores of less than 90 on the Shipley Institute of Living Scale.[24]

Design

Smokers participated in the following 2 imaging sessions: after 24 hours of biochemically confirmed abstinence (carbon monoxide level, <10 ppm) and after smoking as usual (last cigarette about 20 minutes before the scan). Sessions were performed 1 to 3 weeks apart in counterbalanced order. Participants refrained from use of alcohol or other drugs for at least 24 hours before sessions, confirmed by results of a urine drug screen and a breath test for alcohol. Severity of nicotine dependence was assessed by the Fagerström Test for Nicotine Dependence (FTND).[25] The Minnesota Nicotine Withdrawal Scale,[26] the brief Questionnaire on Smoking Urges (QSU),[27] and the Positive and Negative Affect Schedule[28] were administered before each scan. Subjects underwent a 5-minute high-resolution anatomical scan, a 6-minute resting scan, and a 15-minute visual N-back WM task.[8] Unless otherwise specified, data are expressed as mean (SD).

Functional Magnetic Resonance Imaging Data

Data were collected on a commercially available scanner (3T Trio; Siemens). Participants were instructed to relax and lie still with their eyes focused on a central white cross on a black screen during the resting scan. Whole-brain blood oxygenation level–dependent (BOLD) functional magnetic resonance imaging data were acquired using a single-shot gradient-echo echo-planar sequence with the following parameters: 3000/32 milliseconds of repetition/echo times, 90° flip angle, 192 × 192 mm^2 field of view, 64 × 64 matrix, and 3/0-mm slice thickness/gap. For spatial normalization purposes, high-resolution T1-weighted anatomical images were acquired.

Data preprocessing (using AFNI software[29]) included slice timing and motion correction, spatial normalization to Talairach space with a resampled resolution of 3 × 3 × 3 mm^3, nonlinear registration,[30] quadratic detrending, gaussian spatial smoothing (full width half maximum, 6 mm), and mean-based intensity normalization. Mean relative head movement ($||motion||_2$) was evaluated with the following mean Euclidean norm of the 6-motion parameter derivatives:

$$||motion||_2 = \frac{1}{N}\sum_{i=1}^{N}||motion_i||_2$$

where

$$||motion_i||_2 = \sqrt{\Delta d_{ix}^2 + \Delta d_{iy}^2 + \Delta d_{iz}^2 + \Delta\alpha_i^2 + \Delta\beta_i^2 + \Delta\gamma_i^2}$$

The rotational displacements were converted from radians to millimeters by calculating displacement on the surface of a sphere with a radius of 60 mm. We excluded participants with excessive head motion, including 14 during the resting scan and 6 during the WM task scan (including 4 with overlap from the resting scan) ($||motion||_2$, > 0.25 mm). We also excluded 1 participant with poor WM task accuracy (>2.5 SD below the mean), leaving 37 participants (including 19 women) in the analysis. Mean (SD) head movement was 0.11 (0.05) mm (during abstinence) and 0.09 (0.05) mm (during smoking).

Excessive head motion can induce spurious correlation structures in resting connectivity analysis.[31-33] Thus, we used several steps to minimize the influence of head motion, including (1) stringent movement criteria to exclude subjects with mean $||motion||_2$ greater than 0.25 mm, (2) censoring of data points when $||motion_i||_2$ was greater than 0.4 mm, and (3) including mean $||motion||_2$ as a covariate.

Resting Functional Networks

We applied group independent component analysis (GICA) to the resting data using MELODIC (FMRIB Analysis Group, Oxford University).[34,35] The preprocessed data in Talairach space from both sessions were submitted to MELODIC using the command-line tool with the component number set at 20 and the decomposition approach set as temporal concatenation. The GICA spatial maps were converted to z score maps and then thresholded via a mixture model fit to identify voxels contributing to each independent component.[35] The SN, DMN, and ECN were identified by visual inspection of the thresholded GICA maps.[15,17] The similarity in the spatial extent between the identified networks and previously published results[34] was assessed using spatial cross-correlation. Spatial cross-correlation of the SN, ECN, and DMN (transformed to the Montreal Neurological Institute space) with maps described by Beckmann et al[34] show that the identified ECNs are consistent with their frontoparietal network, whereas our SN is spatially consistent with their ECN.

Using the GICA component maps as spatial predictors for each participant's 4-dimensional data, a linear regression generated a time course for each component. As a measure of cross-network coupling, we calculated correlation coefficients (CC) between component time courses derived from the SN, ECN, and the DMN ($CC_{SN,ECN}$ and $CC_{SN,DMN}$). To assess the actions of the SN on DMN and ECN in the smoking and abstinence states with a single value, we defined a composite network association index as $m = z_{SN,ECN} - z_{SN,DMN} = f(CC_{SN,ECN}) - f(CC_{SN,DMN})$, where

$$f(CC) = \frac{1}{2}\ln\left(\frac{1+CC}{1-CC}\right)$$

and m refers to the RAI. The negative sign in front of the SN-DMN correlation ($z_{SN,DMN}/CC_{SN,DMN}$) inverts the negative SN-DMN correlation so that the SN-ECN and SN-DMN correlation strength is added up rather than cancelled out. Large RAI values are taken to reflect a high degree of synchronization of the SN with the ECN and/or DMN, with positive correlation between the SN and ECN and negative correlation between the SN and DMN.

RAI Analyses

Linear mixed-effects modeling (SPSS, version 20.0; IBM Corporation) tested session effects, including age, years of smoking, FTND, IQ, and mean relative head motion as covariates. The relationship between changes of subjective withdrawal and craving and changes of the RAI (smoking vs abstinence states) was investigated using the following regression model:

$$\Delta Y_{a-s} = \beta_0 + \beta_1 \Delta m_{a-s} + \beta_2 \cdot age + \beta_3 \cdot Smoking\ Year + \beta_4 \cdot FTND + \beta_5 \cdot IQ + \beta_6 \cdot \Delta motion_{a-s} + \varepsilon$$

where ΔY_{a-s} is the arithmetic difference of the Minnesota Nicotine Withdrawal Scale withdrawal score or the brief QSU score between the abstinent and smoking states, and Δm_{a-s} is the difference of the RAI between the 2 states.

The relationship between changes in the RAI and changes in WM task performance (accounting for memory load) was investigated using a repeated-measures general linear model controlling for age, years of smoking, FTND, IQ, and head motion. Changes in WM task performance on the 4 task conditions (0-, 1-, 2-, and 3-back) were measured by median correct response time (ΔRT_{a-s}) and d prime ($\Delta d'_{a-s}$), a measurement of accuracy (z value of hit rate minus false alarm rate).[36]

The correlation between the RAI and the WM task activation changes was investigated as in the performance model. The task-induced BOLD signal percentage change (dS/S) for each memory load was extracted from 5 regions of interest identified by a 2 (state) × 4 (memory load) analysis of variance, where

$$\frac{dS_n}{S} = \frac{S_{a,n} - S_0}{S_0} = \frac{\beta_{a,n}}{\beta_{o,n}} \times 100\%,$$

$n = 0b, 1b, 2b, 3b$; $S_{a,n} = \beta_{a,n}p(t) + \beta_{o,n} + \varepsilon$; and $p(t)$ is the paradigm for the WM task. The 5 regions of interest consisted of 3 "task-positive" regions (dorsal anterior cingulate cortex [Talairach coordinates 0, 20, 43] and bilateral DLPFC [left, −44, 24, 23; right, 42, 30, 24], component regions seen in SN and ECN) and 2 "task-negative" regions (ventromedial prefrontal cortex [VMPFC] [−2, 40, −7] and PCC [−6, −55, 21], canonical DMN regions).[6] The WM-related BOLD contrasts were normalized by subtracting the 0-back contrast from each load condition (ie, 1b − 0b, 2b − 0b, and 3b − 0b).

All hypotheses were tested at a global type I error of α = 0.05. Based on the high correlation between left and right hemisphere RAIs (r = 0.65) and the high mean correlation among the 3 subjective measures ($r \approx 0.68$), an adjusted critical α of $P = .04$ was applied to the RAI session effect model and the RAI-subjective measures model. For the RAI-WM task performance and BOLD signal models, an adjusted critical α of $P = .01$ was applied based on the mean correlation between the 5 regions of interest and the 2 task performance measures ($r \approx 0.33$).[37]

Results

Descriptive Data

The 37 smokers (including 19 women) had a mean age of 40.8 (13.2) years (range, 19-61 years) and initiated smoking at 16.5 (3.7) years of age. They smoked a mean of 16.2 (5.1) cigarettes per day, had a mean FTND score of 4.9 (1.6), and smoked for a mean of 24.3 (13.7) years. Mean withdrawal scores (11.5 [8.4]) and urge scores (43.7 [16.4]) in the abstinence state were significantly higher than in the smoking state (3.3 [3.8] and 23.9 [10.8], respectively; $P = .0001$). Negative affect was higher in the abstinence vs smoking states (15.4 [6.6] vs 11.4 [2.5]; $P = .0001$). Abstinence was associated with slower median correct response time ($P = .002$) and lower d prime ($P = .004$).

Resting Networks

Of the 20 GICA components, 4 were identified as SN, ECN, and DMN[15,17] and were thresholded for display at $z = 3.5$ (**Figure 1**). The ECN was decomposed into 2 strongly lateralized components, an observation commonly reported[34,38] and referred to

Figure 1. Functional Magnetic Resonance Images Demonstrating Results of Independent Component Analysis (ICA)

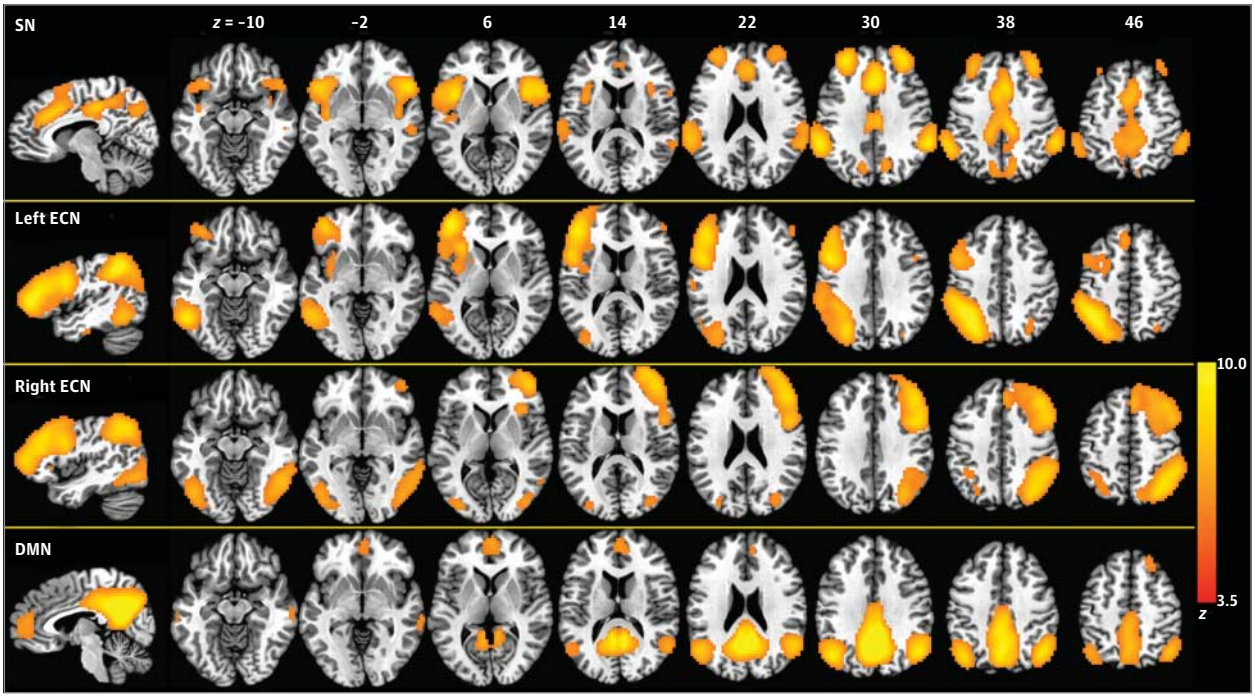

Four networks generated from group ICA of the resting state data were identified as the salience network (SN), default mode network (DMN), and left and right executive control network (ECN). Spatial maps were converted to *z* score images and then thresholded at *z* = 3.5 via a mixture model fit. Network maps are displayed in red-yellow overlaid onto the Talairach standard brain map based on neurological (left = left) convention. Slice coordinates are given in millimeters. The key SN regions included the dorsal anterior cingulate cortex (ACC)/paracingulate gyrus (Talairach coordinates: 3, 21, 33), bilateral anterior insula (left, −39, 9, 3; right, 51, 15, 0), dorsolateral prefrontal cortex (DLPFC) (left, −30, 45, 30; right, 30, 48, 30), supramarginal gyrus (left, −57, −45, 30; right, 57, −42, 33), and precuneus (12, −69, 36). Together, the left and right ECN covered the bilateral DLPFC (Talairach coordinates: left, −42, 45, 6; right, 45, 33, 25), parietal cortices (left, −39, −51, 42; right, 39, −57, 48), middle temporal gyrus (left, −51, −54, −9; right, 51, −57, −9), and dorsal medial frontal gyrus (left, −6, 27, 45; right, 6, 30, 45). The DMN included the posterior cingulate cortex (Talairach coordinates: 6, −57, 27), bilateral angular gyrus (left, −42, −69, 33; right, 48, −63, 30), ventromedial prefrontal cortex/rostral ACC (3, 54, 3), and temporal gyrus (left, −57, −9, −15; right, 60, −18, −15).

as the left ECN (LECN) and right ECN (RECN). Spatial cross-correlation between these networks and previous results[34] revealed a high degree of similarity, with a mean r = 0.55 (range, 0.37-0.65).

Smoking Abstinence Effects

When we considered the LECN and RECN independently, the 2 RAIs were defined corresponding to composite network associations. Because participants showed significantly more relative head motion in the abstinence vs smoking states (P = .02), head motion was included as a covariate in addition to age, years of smoking, FTND, and IQ. The 3-dimensional rendering maps in **Figure 2** illustrate the composition of the RAI in both hemispheres and the change in the RAI between abstinent and smoking states. The RAI decreased significantly in the abstinence compared with the smoking state (left RAI, P = .002; right RAI, P = .04).

The RAI combined SN-ECN and SN-DMN coupling. To better understand which between-network connection was responsible for reducing the RAI during abstinence, we performed post hoc analyses on the session effects of the SN-ECN coupling ($z_{SN,LECN}$ and $z_{SN,RECN}$) and the SN-DMN coupling ($z_{SN,DMN}$), controlling for all the above covariates. The anticorrelation between the SN and DMN was significantly reduced during the abstinence state (P = .02), whereas the correlation between the SN and LECN (P = .04) but not the correlation between the SN and RECN (P = .45) was reduced (**Figure 3**).

Subjective Measures

The change of the right hemisphere RAI (abstinence − smoking) was negatively correlated with changes in smoking urge (r = −0.59; P = .007). Compared with the smoking state, the more the right hemisphere RAI decreased during abstinence, the more urges the subject reported (**Figure 4**). The change in the right hemisphere RAI showed a trend for a similar negative correlation (r = −0.35; P = .09) with withdrawal changes measured by the Minnesota Nicotine Withdrawal Scale. The increase in negative affect showed a nonsignificant negative correlation with RAI change (r = −0.37; P = .09).

Working Memory

We found significant RAI-task activation correlations in all task-negative but not task-positive regions. The decrease of the left hemisphere RAI during the abstinence state predicted less WM task-induced BOLD deactivation in the VMPFC (r = −0.66; P = .003) and PCC (r = −0.65; P = .001; **Figure 5**). No significant interactions of memory load by the RAI on performance or activation were found.

Figure 2. Resource Allocation Index (RAI) in the Abstinence vs Smoking States

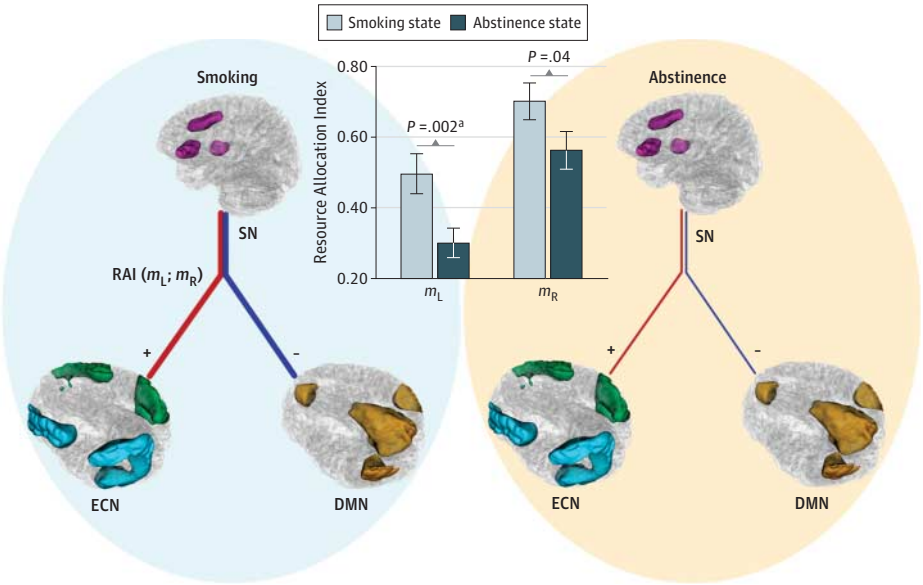

Rendered brain figures present network components identified by group independent component analysis. Compared with the smoking state, the RAI for the left hemisphere (m_L) decreased in abstinence (P = .002); the RAI for the right hemisphere (m_R) showed a decreasing trend (P = .04). A thinner path connecting the salience network (SN) and executive control network (ECN) and the path connecting the SN and default mode network (DMN) in the abstinence (vs smoking) states illustrates decreased coupling between the networks. − Indicates negative correlation; +, positive correlation.
[a]Differences were significant.

Figure 3. Between-Network Coupling in the Abstinence vs Smoking States

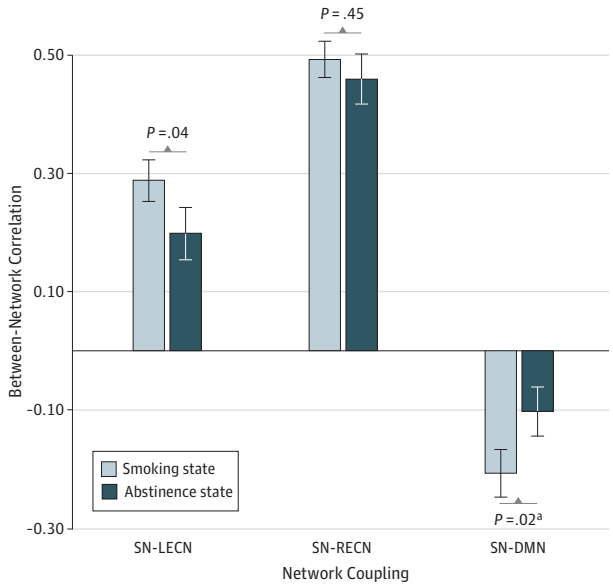

Significant reduction in correlation between the salience network (SN) and default mode network (DMN) (P = .02) in the abstinence vs smoking states. LECN indicates left executive control network; RECN, right executive control network. Whiskers indicate SD.
[a]Differences were significant.

Figure 4. Resource Allocation Index (RAI) Correlation With Smoking Urge Score

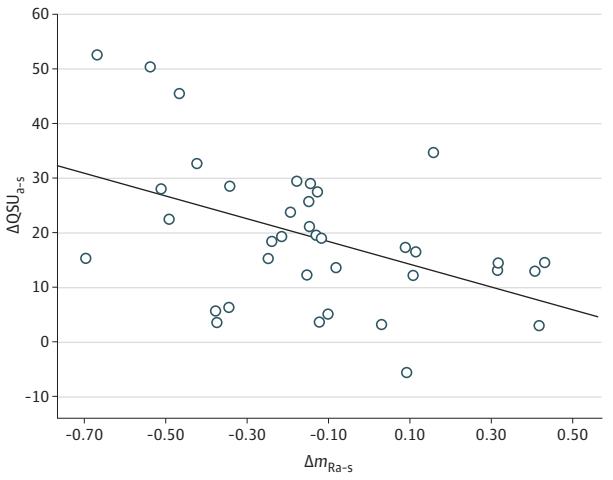

Partial regression plots of the difference of brief Questionnaire on Smoking Urges score between the abstinence and smoking states (ΔQSU_{a-s}) against the difference of the RAI in the right hemisphere between states (Δm_{Ra-s}).

We found a negative trend for an association between the right RAI and WM task performance (r = −0.39; P = .08, controlling for memory load); as the RAI decreased during the abstinence state, the participant responded correctly more slowly. We found no association between the RAI and task accuracy. **Figure 6** summarizes the significant associations between the abstinence-induced changes in the RAI and the abstinence-behavioral and WM-related measures.

Finally, to further instantiate that the RAI has unique merit, we investigated the relationship between $z_{SN,DMN}$ and urge scores and between $z_{SN,DMN}$ and WM task-induced BOLD deactivation. Coupling between the SN and DMN alone did not produce the observed RAI behavioral and neural relationships ($z_{SN,DMN}$ and urge association, P = .38; $z_{SN,DMN}$ and WM-task-induced BOLD deactivation association, P = .59 [VMPFC] and P = .05 [PCC]). These results show the importance of col-

Figure 5. Resource Allocation Index (RAI) Correlations With Working Memory (WM) Task Activation

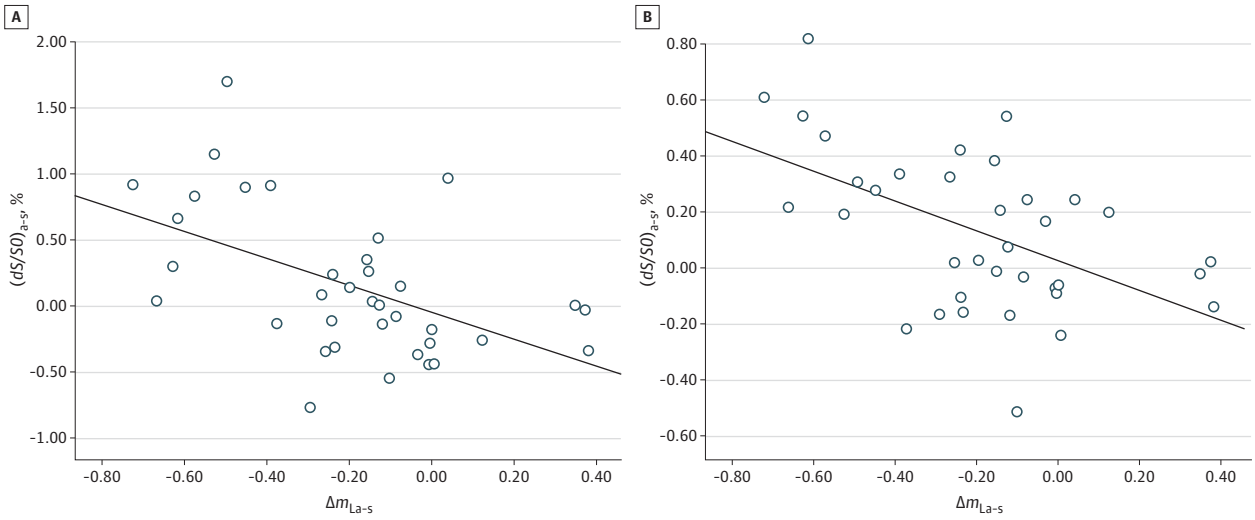

Partial regression plots of the difference between the abstinence vs smoking states of the WM task-induced blood oxygenation level–dependent change ($[dS/SO]_{a-s}$) averaged across memory load in the ventromedial prefrontal cortex (A) and posterior cingulate cortex regions (B) against the difference of the RAI in the left hemisphere ($\Delta m_{L,a-s}$). Markers indicate individual participants.

Figure 6. Schematic of Changes in the Association of the Resource Allocation Index (RAI) Between the Abstinence vs Smoking Sessions

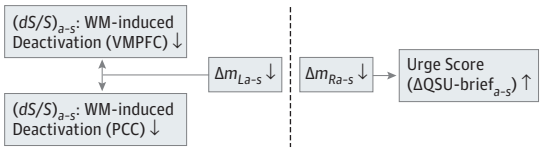

Changes in the working memory (WM)–induced signal percentage change between states ($dS/S)_{a-s}$, the RAI in the right and left hemispheres between states ($\Delta m_{R,a-s}$ and $\Delta m_{L,a-s}$, respectively), and the brief Questionnaire on Smoking Urges (QSU) score between states (ΔQSU_{a-s}) are depicted. PCC indicates posterior cingulate cortex; VMPFC, ventromedial prefrontal cortex. Upward arrow indicates increase; downward arrows, decrease.

lective between-network interactions in accounting for observed behavioral changes.

Discussion

Dysregulated interactions within and between 3 core brain networks (ie, the ECN, DMN, and SN) may underlie neuropsychiatric and addictive disorders.[15,22,39] A composite network association index (the RAI) integrating the SN-ECN and SN-DMN cross-network correlations was developed to assess our network interaction hypothesis. The RAI in smokers was significantly lower in the abstinence compared with the smoking state. Post hoc analyses revealed a significantly weaker (negative) SN-DMN correlation during abstinence, suggesting that weaker inhibition between the DMN and SN was the driving force for the lower RAI. Also, change in the RAI during the abstinence (compared with smoking) state was negatively correlated with changes in smoking urges, suggesting that weaker network connectivity contributes to urges to smoke. Consistently, lower RAI values in the abstinence (compared with smoking) state also predicted less BOLD suppression in task-negative (DMN) regions during WM task performance.

Cognitively demanding tasks activate brain regions within the SN (eg, insula, dorsal anterior cingulate cortex) and ECN (eg, DLPFC) and deactivate regions of the DMN (eg, PCC, VMPFC).[6,19,40] Alterations in coupling between these networks, and specifically the failure to suppress DMN activity, increase the probability of error on cognitive tasks.[41,42] We extend these observations by demonstrating the predictive validity of a novel index (RAI) that combines the SN-DMN and SN-ECN correlation strength additively, thereby reflecting concurrent adjustments in task-positive and task-negative activity that may be attributable to the detection of salient events and modulation of activity via the SN. The RAI should be more sensitive than individual paired network couplings (SN-DMN and SN-ECN), provided that the noise probability distribution functions in the individual indexes are not fully dependent.

The strong negative correlation between changes in the RAI and changes in urges to smoke and the association of RAI reductions with failed suppression of DMN activity during a WM task suggest that concurrent alteration of SN-DMN and SN-ECN couplings may be integral in processing divided attentional resources, cognitive functions, and, in this instance, a clinically relevant symptom of nicotine withdrawal. Further, although many studies[43,44] have reported lateralized prefrontal functions, the data-driven GICA not only identified lateralized coherence patterns for the ECN, but the lateralized RAI indicated that each predicted independent but related functions. The RAI for the left hemisphere predicted changes in WM BOLD imaging; for the right hemisphere, changes in craving.

These findings further our understanding of aberrant neural mechanisms underlying cognitive deficits observed in ab-

staining smokers[1,2] and how these deficits may increase relapse risk.[4,5] We propose that in the nicotine-deprived state, the SN increases the allocation of attentional resources to attend to abstinence-induced cravings to smoke, leading to a bias toward enhanced DMN activity (ie, decreased inhibition of the DMN). Concurrently, weaker SN-ECN coupling during abstinence decreases ECN operations. The combination of decreased ECN activity and less suppression of DMN activity may result in cognitive deficits.[22,45] Moreover, reductions in ECN activity may increase smokers' difficulty in exerting top-down cognitive control to resist urges to smoke.

In addition, abstinence-induced alterations in SN-DMN coupling might relate to dysphoria associated with nicotine withdrawal. Smokers exhibited significant increases in negative mood symptoms in the abstinence vs smoking states, and the reduction in the RAI in abstinence (vs smoking) showed a trend for association with increased negative affect. Likewise, patients with depression and dysthymia show increases in resting-state DMN activity and altered DMN connectivity compared with control patients,[46,47] an effect normalized by antidepressant treatment.[46] These abnormalities in resting-state connectivity are thought to contribute to DMN hyperactivity and an inability to shift attention away from ruminations that characterize these disorders. Thus, we speculate that smokers attempting to quit may also experience difficulty disengaging from self-focused thoughts related to withdrawal discomfort, as reflected in the weaker SN-DMN anticorrelation in the RAI.

Despite the strengths of this study, including the relatively large sample size and within-subject design, these data should be interpreted in light of potential limitations. The RAI was based on a hypothesized model of abstinence-induced network interactions leading to cognitive deficits; we did not explore whether other network components contribute to the model. The abstinence manipulation to induce alterations in the RAI was performed at a single time and should be manipulated parametrically. The RAI could also be applied in other dysregulated states and related to functional magnetic resonance imaging data acquired from a variety of tasks. If the RAI is to be applied as a diagnostic biomarker, test-retest studies (as previously demonstrated with GICA reliability assessments[48-50]) are needed to demonstrate its reproducibility and clinical significance.

Additional technical issues need to be considered. The RAI was defined based on the results from the data-driven GICA analysis using a 20-component solution. We also performed GICA using component numbers of 25 and 30. The mean spatial cross-correlation between the visually identified DMN, SN, and ECN components and those previously published[34] did not significantly differ as a function of dimensionality ($P > .50$). All of our subsequent RAI calculations and analyses were based on network maps with the component number set at 20. In addition to differences in the literature on the spatial extent of network components, the nomenclature differs. For example, what we call the ECN has also been labeled the central executive network[15] and the frontal-parietal network.[11] Their spatial extents are similar and all are task-positive networks; the interchangeability of names does not alter the significance of our findings. Finally, the RAI was based on a specific 3-network interaction model.[22] Additional networks may also contribute to the abstinence mechanism.

Despite these limitations, the present findings point to a novel pathophysiological mechanism underlying nicotine withdrawal symptoms that promote smoking relapse. These data move beyond the concept of a dysregulated DMN to suggest that the ability of the SN to toggle (or perhaps rapidly oscillate) between the ECN and the DMN, along with the ability to disengage from DMN activity, may be critical in cognitive alterations that underlie nicotine addiction. Because successful quitting requires top-down executive cognitive control over smoking urges, exploration of the relationship of the RAI to quitting success in a longitudinal cohort study would be important. On validation, the RAI could serve as a clinical biomarker to identify smokers who are most likely to respond to a particular treatment. For example, evidence that antidepressant treatment normalizes altered resting-state DMN connectivity among patients with dysthymia[46] suggests that smokers who exhibit abstinence-induced reductions in the RAI may benefit from the antidepressant bupropion hydrochloride for smoking cessation. With additional validation in other cohorts, the RAI could also be a potential biomarker for screening novel treatments for smoking cessation.[51]

Conclusions

Alterations in SN-DMN coupling and the inability to disengage from the DMN may be critical in cognitive/affective alterations that underlie nicotine dependence. Further studies may validate the use of the RAI as a potential biomarker to identify smokers most likely to respond to a particular cessation therapy.

ARTICLE INFORMATION

Submitted for Publication: April 9, 2013; final revision received and accepted September 9, 2014.

Published Online: March 12, 2014. doi:10.1001/jamapsychiatry.2013.4091.

Author Contributions: Drs Lerman and Stein had full access to all the data in the study and take responsibility for the integrity of the data and the accuracy of the data analysis.
Study concept and design: Lerman, Loughead, Ruparel, Yang, Stein.
Acquisition, analysis, or interpretation of data: All authors.
Drafting of the manuscript: Lerman, Gu, Stein.
Critical revision of the manuscript for important intellectual content: Gu, Loughead, Ruparel, Yang, Stein.
Statistical analysis: Gu, Ruparel, Yang, Stein.
Obtained funding: Lerman, Loughead, Stein.
Administrative, technical, or material support: Gu, Loughead, Yang, Stein.
Study supervision: Loughead, Yang, Stein.

Conflict of Interest Disclosures: Dr Lerman has received research funding from Pfizer independent of this research project. No other disclosures were reported.

Funding/Support: This study was supported by grants P50 CA143187 and R03 DA027438 (Dr Lerman), the Intramural Research Program of the National Institute on Drug Abuse (Dr Stein), and the Commonwealth of Pennsylvania Department of Health.

Role of the Sponsor: The funding sources had no role in the design and conduct of the study; collection, management, analysis, and interpretation of the data; preparation, review, or approval of the manuscript; and decision to submit the manuscript for publication.

Additional Contributions: James Loughead, PhD, Ruben Gur, PhD, and E. Paul Wiley, PhD, assisted in the design of the original study. Leah La Prate, Mary Falcone, PhD, Christopher Jepson, PhD, and Susan Ware, BA, contributed data set creation and data management.

REFERENCES

1. Evans DE, Drobes DJ. Nicotine self-medication of cognitive-attentional processing. *Addict Biol*. 2009;14(1):32-42.

2. Myers CS, Taylor RC, Moolchan ET, Heishman SJ. Dose-related enhancement of mood and cognition in smokers administered nicotine nasal spray. *Neuropsychopharmacology*. 2008;33(3):588-598.

3. Patterson F, Jepson C, Strasser AA, et al. Varenicline improves mood and cognition during smoking abstinence. *Biol Psychiatry*. 2009;65(2):144-149.

4. Dolan SL, Sacco KA, Termine A, et al. Neuropsychological deficits are associated with smoking cessation treatment failure in patients with schizophrenia. *Schizophr Res*. 2004;70(2-3):263-275.

5. Patterson F, Jepson C, Loughead J, et al. Working memory deficits predict short-term smoking resumption following brief abstinence. *Drug Alcohol Depend*. 2010;106(1):61-64.

6. Falcone M, Wileyto EP, Ruparel K, et al. Age-related differences in working memory deficits during nicotine withdrawal [published online March 18, 2013]. *Addict Biol*. doi:10.1111/adb.12051.

7. Hahn B, Ross TJ, Yang Y, Kim I, Huestis MA, Stein EA. Nicotine enhances visuospatial attention by deactivating areas of the resting brain default network. *J Neurosci*. 2007;27(13):3477-3489.

8. Loughead J, Ray R, Wileyto EP, et al. Effects of the α4β2 partial agonist varenicline on brain activity and working memory in abstinent smokers. *Biol Psychiatry*. 2010;67(8):715-721.

9. Tanabe J, Nyberg E, Martin LF, et al. Nicotine effects on default mode network during resting state. *Psychopharmacology (Berl)*. 2011;216(2):287-295.

10. Fox MD, Greicius M. Clinical applications of resting state functional connectivity. *Front Syst Neurosci*. 2010;4:19. doi:10.3389/fnsys.2010.00019.

11. Smith SM, Fox PT, Miller KL, et al. Correspondence of the brain's functional architecture during activation and rest. *Proc Natl Acad Sci U S A*. 2009;106(31):13040-13045.

12. Wylie KP, Rojas DC, Tanabe J, Martin LF, Tregellas JR. Nicotine increases brain functional network efficiency. *Neuroimage*. 2012;63(1):73-80.

13. Zou Q, Ross TJ, Gu H, et al. Intrinsic resting-state activity predicts working memory brain activation and behavioral performance. *Hum Brain Mapp*. 2013;34(12):3204-3215.

14. Gusnard DA, Akbudak E, Shulman GL, Raichle ME. Medial prefrontal cortex and self-referential mental activity. *Proc Natl Acad Sci U S A*. 2001;98(7):4259-4264.

15. Menon V. Large-scale brain networks and psychopathology: a unifying triple network model. *Trends Cogn Sci*. 2011;15(10):483-506.

16. Raichle ME, MacLeod AM, Snyder AZ, Powers WJ, Gusnard DA, Shulman GL. A default mode of brain function. *Proc Natl Acad Sci U S A*. 2001;98(2):676-682.

17. Seeley WW, Menon V, Schatzberg AF, et al. Dissociable intrinsic connectivity networks for salience processing and executive control. *J Neurosci*. 2007;27(9):2349-2356.

18. Sridharan D, Levitin DJ, Menon V. A critical role for the right fronto-insular cortex in switching between central-executive and default-mode networks. *Proc Natl Acad Sci U S A*. 2008;105(34):12569-12574.

19. Fox MD, Snyder AZ, Vincent JL, Corbetta M, Van Essen DC, Raichle ME. The human brain is intrinsically organized into dynamic, anticorrelated functional networks. *Proc Natl Acad Sci U S A*. 2005;102(27):9673-9678.

20. Fox MD, Zhang D, Snyder AZ, Raichle ME. The global signal and observed anticorrelated resting state brain networks. *J Neurophysiol*. 2009;101(6):3270-3283.

21. Menon V, Uddin LQ. Saliency, switching, attention and control. *Brain Struct Funct*. 2010;214(5-6):655-667.

22. Sutherland MT, McHugh MJ, Pariyadath V, Stein EA. Resting state functional connectivity in addiction. *Neuroimage*. 2012;62(4):2281-2295.

23. Sheehan DV, Lecrubier Y, Sheehan KH, et al. The Mini-International Neuropsychiatric Interview (M.I.N.I.). *J Clin Psychiatry*. 1998;59(suppl 20):22-57.

24. Zachary R. *Shipley Institute of Living Scale–Revised Manual*. Los Angeles, CA: Western Psychological Services; 2000.

25. Heatherton TF, Kozlowski LT, Frecker RC, Fagerström KO. The Fagerström Test for Nicotine Dependence. *Br J Addict*. 1991;86(9):1119-1127.

26. Hughes JR, Hatsukami DK, Pickens RW, Krahn D, Malin S, Luknic A. Effect of nicotine on the tobacco withdrawal syndrome. *Psychopharmacology (Berl)*. 1984;83(1):82-87.

27. Cox LS, Tiffany ST, Christen AG. Evaluation of the brief Questionnaire of Smoking Urges (QSU-brief) in laboratory and clinical settings. *Nicotine Tob Res*. 2001;3(1):7-16.

28. Watson D, Clark LA, Tellegen A. Development and validation of brief measures of positive and negative affect: the PANAS scales. *J Pers Soc Psychol*. 1988;54(6):1063-1070.

29. Cox RW. AFNI: software for analysis and visualization of functional magnetic resonance neuroimages. *Comput Biomed Res*. 1996;29(3):162-173.

30. Geng X, Christensen GE, Gu H, Ross TJ, Yang Y. Implicit reference-based group-wise image registration and its application to structural and functional MRI. *Neuroimage*. 2009;47(4):1341-1351.

31. Power JD, Barnes KA, Snyder AZ, Schlaggar BL, Petersen SE. Spurious but systematic correlations in functional connectivity MRI networks arise from subject motion. *Neuroimage*. 2012;59(3):2142-2154.

32. Satterthwaite TD, Wolf DH, Loughead J, et al. Impact of in-scanner head motion on multiple measures of functional connectivity. *Neuroimage*. 2012;60(1):623-632.

33. Van Dijk KR, Sabuncu MR, Buckner RL. The influence of head motion on intrinsic functional connectivity MRI. *Neuroimage*. 2012;59(1):431-438.

34. Beckmann CF, DeLuca M, Devlin JT, Smith SM. Investigations into resting-state connectivity using independent component analysis. *Philos Trans R Soc Lond B Biol Sci*. 2005;360(1457):1001-1013.

35. Beckmann CF, Smith SM. Probabilistic independent component analysis for functional magnetic resonance imaging. *IEEE Trans Med Imaging*. 2004;23(2):137-152.

36. Haatveit BC, Sundet K, Hugdahl K, Ueland T, Melle I, Andreassen OA. The validity of d prime as a working memory index. *J Clin Exp Neuropsychol*. 2010;32(8):871-880.

37. Sankoh AJ, Huque MF, Dubey SD. Some comments on frequently used multiple endpoint adjustment methods in clinical trials. *Stat Med*. 1997;16(22):2529-2542.

38. Gordon EM, Stollstorff M, Devaney JM, Bean S, Vaidya CJ. Effect of dopamine transporter genotype on intrinsic functional connectivity depends on cognitive state. *Cereb Cortex*. 2012;22(9):2182-2196.

39. Liston C, Malter Cohen M, Teslovich T, Levenson D, Casey BJ. Atypical prefrontal connectivity in attention-deficit/hyperactivity disorder. *Biol Psychiatry*. 2011;69(12):1168-1177.

40. Lawrence NS, Ross TJ, Hoffmann R, Garavan H, Stein EA. Multiple neuronal networks mediate sustained attention. *J Cogn Neurosci*. 2003;15(7):1028-1038.

41. Eichele T, Debener S, Calhoun VD, et al. Prediction of human errors by maladaptive changes in event-related brain networks. *Proc Natl Acad Sci U S A*. 2008;105(16):6173-6178.

42. Prado J, Carp J, Weissman DH. Variations of response time in a selective attention task are linked to variations of functional connectivity in the attentional network. *Neuroimage*. 2011;54(1):541-549.

43. Stephan KE, Fink GR, Marshall JC. Mechanisms of hemispheric specialization. *Neuropsychologia*. 2007;45(2):209-228.

44. Stephan KE, Marshall JC, Friston KJ, et al. Lateralized cognitive processes and lateralized task control in the human brain. *Science*. 2003;301(5631):384-386.

45. Fox MD, Raichle ME. Spontaneous fluctuations in brain activity observed with functional magnetic resonance imaging. *Nat Rev Neurosci*. 2007;8(9):700-711.

46. Posner J, Hellerstein DJ, Gat I, et al. Antidepressants normalize the default mode network in patients with dysthymia. *JAMA Psychiatry*. 2013;70(4):373-382.

47. Sheline YI, Price JL, Yan Z, Mintun MA. Resting-state functional MRI in depression unmasks increased connectivity between networks via the dorsal nexus. *Proc Natl Acad Sci U S A*. 2010;107(24):11020-11025.

48. Chen S, Ross TJ, Zhan W, et al. Group independent component analysis reveals consistent resting-state networks across multiple sessions. *Brain Res*. 2008;1239:141-151.

49. Damoiseaux JS, Rombouts SA, Barkhof F, et al. Consistent resting-state networks across healthy subjects. *Proc Natl Acad Sci U S A*. 2006;103(37):13848-13853.

50. Zuo XN, Kelly C, Adelstein JS, Klein DF, Castellanos FX, Milham MP. Reliable intrinsic connectivity networks. *Neuroimage*. 2010;49(3):2163-2177.

51. Bough KJ, Lerman C, Rose JE, et al. Biomarkers for smoking cessation. *Clin Pharmacol Ther*. 2013;93(6):526-538.